JOURNAL OF MATERIALS SCIENCE **36** (2001) 3261 – 3271

Non-equilibrium solidification by laser surface alloying of molybdenum with nickel: Structure and properties of alloyed layers

R. PAWLAK
Division of Materials Science and Electrotechnology, Technical University of Lodz, B. Stefanowskiego 18/22, 90-924 Lodz, Poland
E-mail: rypawlak@matel.p.lodz.pl

Z. GAWRONSKI
Institute of Materials Engineering, Technical University of Lodz, B. Stefanowskiego 1/15, 90-924 Lodz, Poland

A. GASSER, K. WISSENBACH
Fraunhofer Institute for Laser Technology, Steinbachstr. 15, 52074 Aachen, Germany

Surface alloying was carried out on molybdenum using continuous wave Nd : YAG and CO_2 lasers. The alloying element (nickel) was deposited on the molybdenum surface by plasma spraying. Microstructure evolution and phase identification was investigated by means of optical and scanning microscopy and X-ray microanalysis. Layers with an average content of about 33% at. of nickel were obtained. Rapid solidification with fine scale microstructures and non-equilibrium nickel rich phases was reported. Molybdenum oxides with a suggested composition of the MoO_2 were also identified. In addition the results of investigations of the alloyed layer microhardness and the layer resistance to erosion in an electric arc have been presented.

1. Introduction

Surface treatment technologies employing a laser beam, including laser alloying, are successfully used to improve such qualities of the surface layer as wear, heat and corrosion resistance in aggressive media [1–5]. By using metal surface layer laser alloying, electrical properties of a metal can be modified, including the formation of a contact material of an increased erosion resistance in an electric arc [6]. A laser beam has been used, among other things, for surface alloying of high-melting metals, such as Mo, W, Ti [7]. The introduction of nickel into the molybdenum surface layer is one method of activating metal surfaces to obtain good metal-ceramics joints [8, 9]. Surface modification can facilitate the bonding of high-melting metals with metals that do not form solid solutions and intermetallic phases [6]. A laser beam is also employed to improve the quality of plasma sprayed layers that contain, among other things, nickel and molybdenum [3]. The surface layer can undergo laser fusion both in the process of spraying [4], and in the course of a plasma process [5]. In the present work, the results have been presented of investigations into the structure of the layers obtained in a process of laser alloying of molybdenum with nickel using continuous lasers: CO_2 and Nd : YAG. An attempt has also been presented at a description of how the structure being formed affects functional properties of the alloyed layer, including erosion in an electric arc.

2. Rapid solidification during laser alloying

The laser alloying process is characterized by the rapid fusion of a small volume of the metal surface layer. During this process both the base and an alloying metal, which has already been deposited onto the surface under treatment or is being introduced into the fusion zone in the course of the process, are fused. In the molten pool, dynamic processes of thermocapillary convection occur, causing the motion of the molten metal and contributing to the homogenizing of the composition [7, 10, 11]. The termination of the laser beam action on a given fragment of the surface under treatment brings about a process of rapid cooling and high-rate crystallization, which results in the formation—in the alloyed layer—of fine-grained microstructures, metastable phases and extended solubility solutions in the solid state [2, 3]. At a high rate of solidification, banded structures are formed, observed—among other things—in Al-Fe or Ag-Cu systems [11, 12]. Extremely high solidification rates lead to the amorphization of the metal surface layer [2]. A large number of cases of laser alloying of different metals have been studied, in which the effects of rapid crystallization were observed, described e.g. in [2, 11, 12]. Theoretical models of rapid solidification of diluted and concentrated alloys [13] have been developed. The kind of structures formed in a laser alloying process depends on many factors, the most important being alloy composition and

solidification rate. If the velocity of diffusion of the atoms dissolved is lower than the velocity of shift of the liquid-solid boundary, then metastable solutions of concentrations exceeding equilibrium solubility limits are formed.

3. Experimental procedure

Laser surface alloying of molybdenum with nickel was carried out using two types of continuous lasers:

a Nd : YAG laser cw (NEC) of a beam power adjustable in the range of 0.05–1.0 kW and the diameter of a focused beam of 0.4–2.5 mm — ***A*** type layers,

CO_2 (cw) TRUMPF of a beam power adjustable in the range of 1.5–7.5 kW focused to the area of a 1 × 6-mm rectangle — ***B*** type layers.

The optimal parameters of the laser alloying process for producing ***A*** and ***B*** layers are shown in Table I.

The formation of Mo-Ni layers by means of a continuous laser beam causes problems resulting from the physical-thermal properties of both metals. The boiling point of nickel (3198°C) is only slightly higher than the melting point of molybdenum (2893°C). Thus increasing the power to obtain alloyed layers of a greater depth leads quickly to the destabilization of the process and rapidly developing hydrodynamic phenomena in the fusion pool. ***A*** type layers were made using the sequence of treatment shown in Fig. 1.

B type layers (a CO_2 laser) were formed as a result of interaction of a beam focused with a linear mirror to the area of a 6 × 1-mm rectangle, at a scanning rate greater than for ***A*** layers. A further increase in the beam power (above 4.3 kW) led to the ignition of plasma. The alloying material (nickel) was preliminarily deposited by plasma spraying in an atmosphere of argon. The thickness of the nickel layer was 90 or 120 μm. The thickness of thus obtained alloyed layers ranged from 250 to 350 μm.

The structure of the layers was investigated by means of optical microscopy (*neophot21*) and electron microscopy (*Hitachi S-4200*) using metallographic sections. The composition of particular phases of the alloyed layers was investigated using X-ray microanalyzers: a *Link II* and a *Voyager 3500* system; the results obtained are identical using the two techniques.

TABLE I The parameters of laser alloying process

Process parameters ⇓ / Layer type ⇒	***A***	***B***
Beam power	0.55 kW	4.3 kW
Scanning rate	25 mm/min	150 mm/min
Interaction area size	$d_0 = 0.8$ mm	1 × 6 mm
Power density	1.1×10^5 W/cm^2	0.8×10^5 W/cm^2
Interaction time	1.9 sec	400 ms

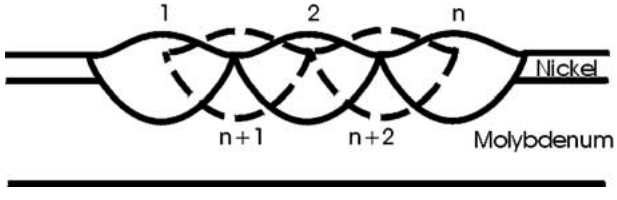

Figure 1 A method of making ***A*** type layers; (1, 2 *n*, *n* + 1, . . .) – sequence of treatment of particular paths.

4. Mo-Ni layer structure

The structure and phase composition of ***A*** type and ***B*** type layers differ because of the formation method and the different kinetics of the alloying process (see Table I). The structure of ***A*** layer is shown in Fig. 2a. The section perpendicular to the direction of treatment manifests typical, cyclic changes in the depth, related to the overlapping of successive laser alloying paths causing partial remelting. This is confirmed by an image of the section parallel to the layer surface (Fig. 2b). Light-coloured, wide bands are the result of alloying in cycles *n*, *n* + 1, etc. (cf. Fig. 1). They are characterized by a distinct dendritic structure. In the path centre, where the crystallization front is the most stable, the dendrites are of considerable size (1–2 mm) and are arranged parallel to the direction of laser beam scanning (Fig. 2c).

Dark bands marked in Fig. 2b are composed of smaller dendrites without any distinct uniform orientation. At the layer bottom, that is on the boundary of the base (Mo)-the alloyed layer, dendrites perpendicular to the crystallization front crystallized epitaxially (Fig. 2d). The inter-dendritic space is filled with a disintegrated eutectic of the plate thickness of an order of 0.7 μm (Fig. 2e).

The composition of dendrites ranges from 2.1 to 5.2 at % Ni, the remaining portion being Mo. It follows from the above that they were formed as a result of non-equilibrium crystallization (Fig. 2f). It was caused by a very high rate of cooling, of an order of 1.2×10^4 K/sec and 1.2×10^4 K/sec, after 1 ms and 10 ms from the termination of the laser beam interaction with a given surface point [7], respectively. The Mo-Ni phase equilibrium system does not virtually show the existence of ε-phase in the solid state at ambient temperature and the greatest solubility of nickel in molybdenum in the liquid phase amounts to 1.8 at % at 1362°C.

In many areas, with greater intensity close to the layer bottom, there occur characteristic arborescent dendrites (Fig. 3a and b), which usually have well-developed arms of the second order. Microanalysis (Fig. 3c) has shown that they are molybdenum oxides of the composition of about 32 at % Mo and 66 at % O, which suggests the MoO_2 composition. The laser alloying process was carried out in a protective atmosphere of Ar. An analysis of the preliminarily deposited nickel layer has confirmed that the structure is characteristic of the plasma sprayed layers. It has shown a significant presence of nickel oxides containing about 20 at % oxygen (Fig. 4a) at an average content of oxygen in the plasma layer of around 4.5 at % (Fig. 4b). An additional analysis by means of an X-ray spectrometer has confirmed these results. They follow from the rudiments of the theory of diffusion and oxidation of metals [14] that molybdenum manifests a clearly closer affinity to oxygen than nickel. During the laser treatment, nickel oxides disintegrated, and the liberated oxygen reacted with molybdenum.

The structure of ***B*** type layers is more homogeneous (Fig. 5a), since they were formed as a result of single scanning with a linearly focused beam. A thin layer of a non-equilibrium solution of a content of about 5.5 at % Ni (Fig. 5b) crystallized directly from the base. The structure of the remaining part of the alloyed layer is made up of equiaxial dendrites, which developed at the bottom of the melt pool and directed perpendicular to the molybdenum-layer boundary (Fig. 5b). In the case of ***B*** type layers, the composition of the dendrites, containing from approx. 4 to 8 at % Ni, also testifies to the non-equilibrium crystallization of the alloyed layer (Fig. 5c). The inter-dendritic space is occupied by a regularly arranged eutectic of tiny plates (Fig. 5d). The Mo-Ni eutectic contains an average of 38 at % Mo, its lighter-coloured skeleton being more abundant in molybdenum (45 at %) than the dark plates (33 at %).

Furthermore, arborescent dendrites of molybdenum oxides occur in the structure. The layers made with a CO_2 laser contain many spheroidal regions of a complex structure. These regions crystallized initially,

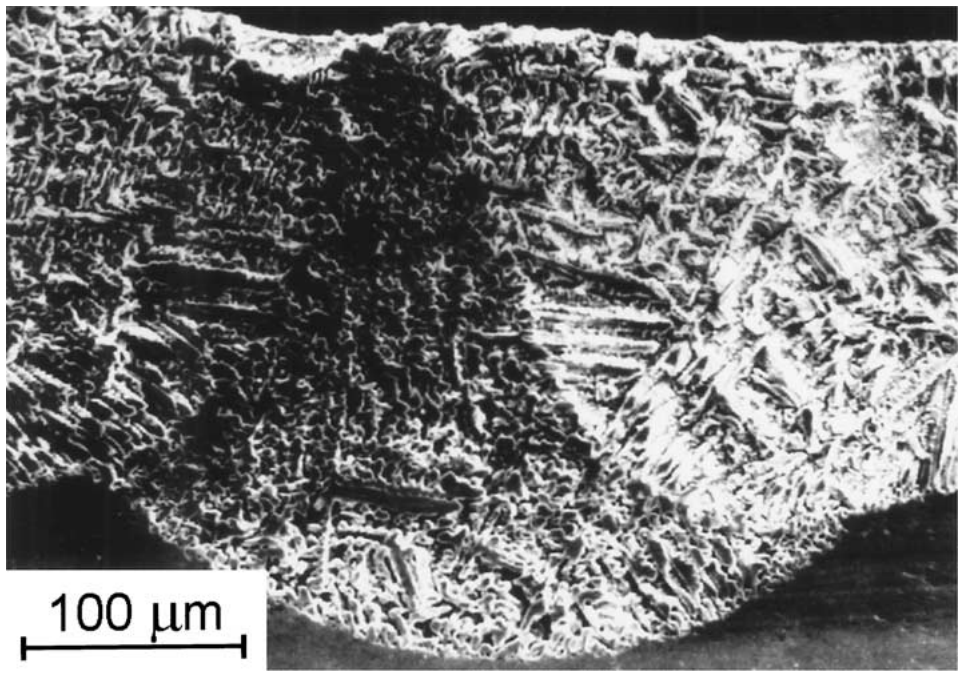

(a)

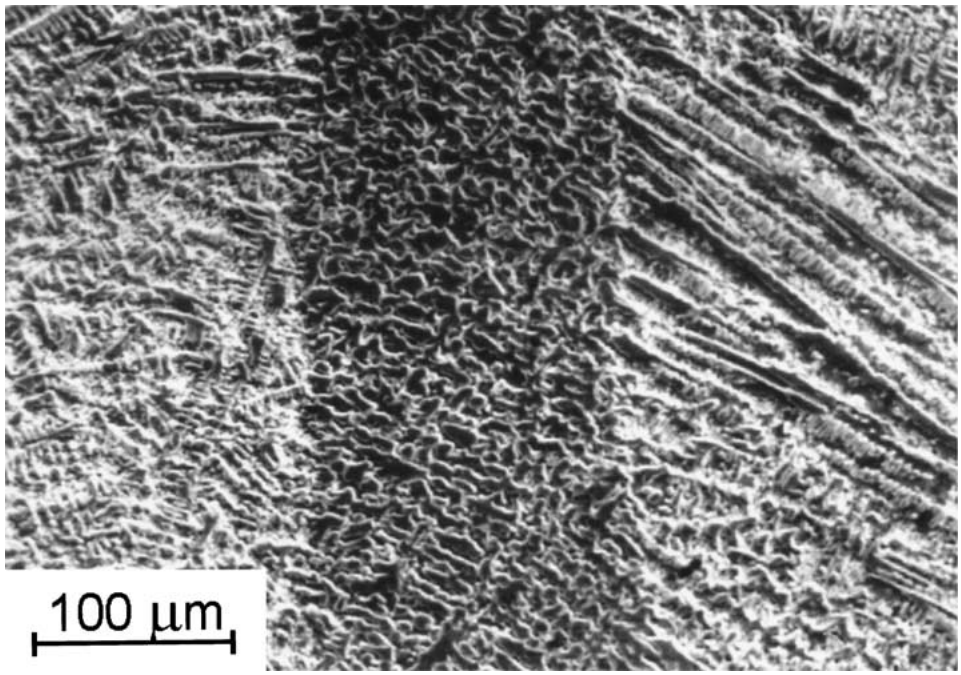

(b)

Figure 2 The structure of Mo layers alloyed with Ni using an Nd : YAG laser: (a, b) - cyclic changes in the structure of Mo-Ni layers of A type; (a) – perpendicular section; (b) – section parallel to the layer surface; (c) – large dendrites in the centre of laser beam scanning path; (d) – dendrites crystallizing perpendicular to the crystallization front; (e) – an eutectic of layers alloyed with an Nd : YAG cw laser; (f) – an EDX spectrum indicating the analysis of composition of non-equilibrium dendrites of phase *ε (Continued)*.

initiating the crystallization of non-equilibrium dendrites of the Mo-Ni solution (Fig. 6a and b).

The course of crystallization in both cases (***A*** and ***B***) is similar. The action of a laser beam results, in the first stage, in the melting of the plasma sprayed coating (Ni) and then of the base material (Mo). Convection currents occur in the fusion, contributing to the homogenization of the composition. Under the conditions of stationary melting with a beam scanned over the surface, in the molten pool a temperature field of such a shape is formed that the lowest crystallization rate is at the bottom of the fusion zone and it increases towards the free surface. This causes a flat crystallization front to be formed at the bottom of the alloyed layer, as a result of which a thin layer of the non-equilibrium ε phase crystallize on the boundary with the base. Non-equilibrium dendrites of the ε phase crystallizes from the base and in the volume of the fusion zone at a later stage. Spheroidal regions containing molybdenum oxides that solidify earlier, and are conducive to the crystallization of dendrites of the ε phase, play an essential role in the crystallization of ***B*** type layers. In the vicinity of the layer surface, the dendritic phase is oriented corresponding to the movement of a laser beam, which is distinct in ***A*** type layers formed at lower scanning speeds, that is to say, in the conditions of greater stability of the crystallization front. Dendrites on the edges of the path are oriented roughly perpendicular to the

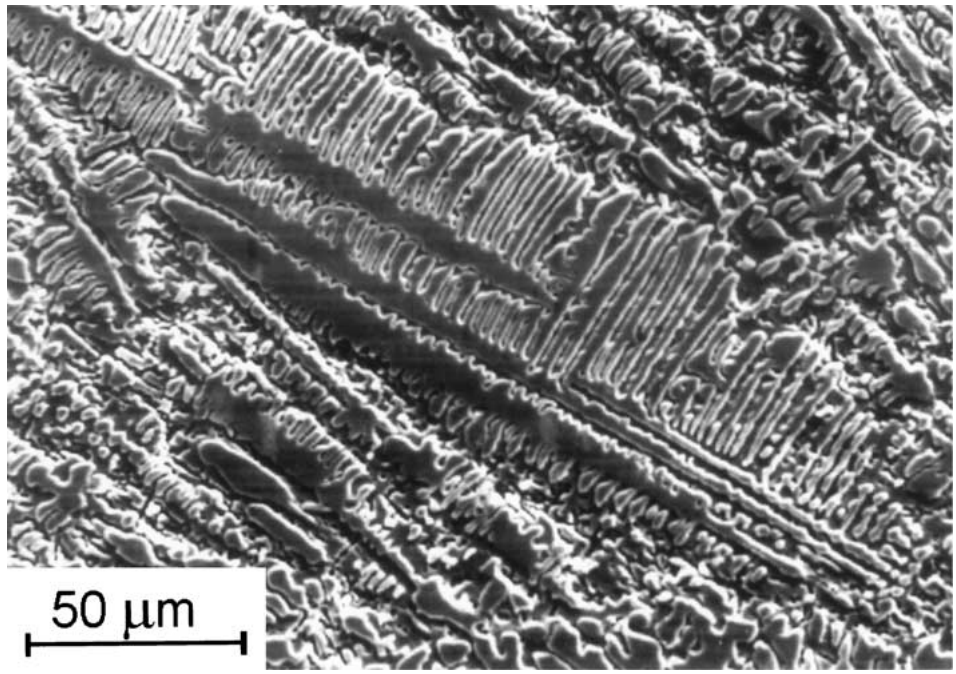

(c)

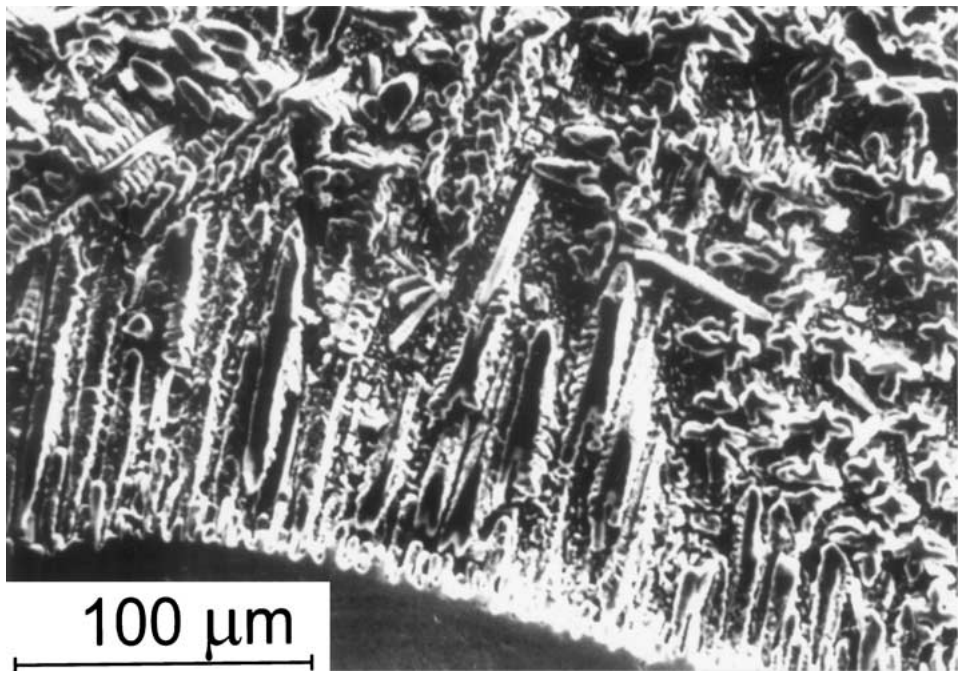

(d)

Figure 2 (Continued).

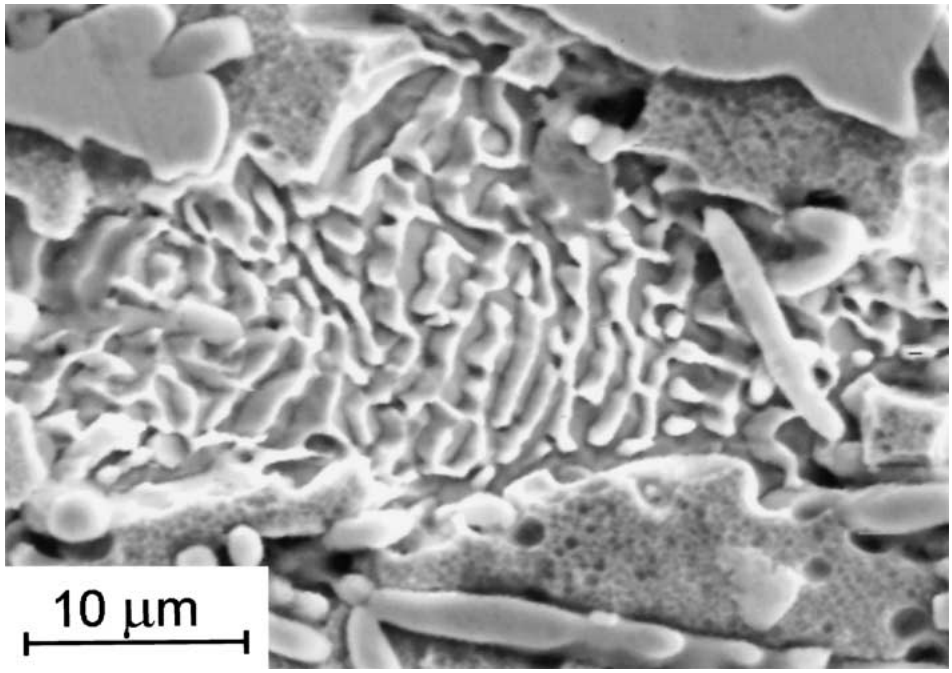

(e)

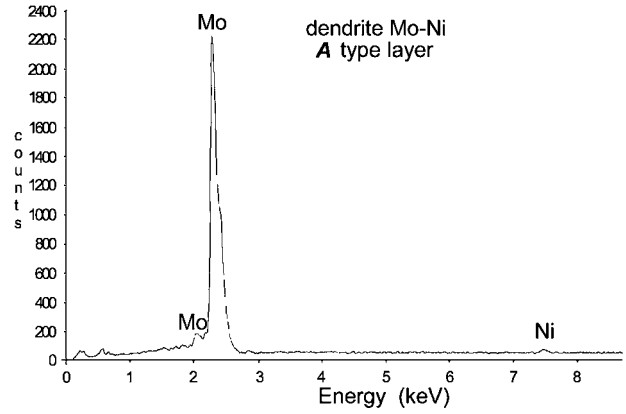

(f)

Figure 2 (Continued).

fusion boundary and reflect the direction of the temperature gradient. At the final stage of solidification there occurs the crystallization of the eutectic phase in the interdendritic spaces.

In spite of not very high relative scanning rates of a beam (in practice the motion of the work table x-y), high values of the surface power density (1.1×10^5 W/cm^2 for ***A*** layers and 0.8×10^5 W/cm^2 for ***B*** layers) and considerable rates of cooling were achieved due to the small beam dia. used. Such a rate of cooling contributes to the crystallization of dendrites of a definitely non-equilibrium composition, with small gaps of arms of the second order. The great refinement of eutectics, in which the plate thickness does not exceed 0.5 μm, although the eutectic phase is formed at the final stage of solidification when the rate of crystallization diminishes, also testifies to the high rates of crystallization.

Since ***A*** type layers were formed as a result of the overlapping of the adjacent paths of laser treatment, and consequently remelting of part of the initial series of tracks, areas of a different content of nickel occur in them. The characteristic, bright areas in Fig. 2a and b were formed during the second series of scanning (see Fig. 1), as a result of the repeated alloying of the initially alloyed areas obtained in the first series of scanning. The average content of nickel in these areas is of an order of 32 at %, while in the dark areas it is about 15 at %.

5. Properties of alloyed layers

The aim of our investigations was among other things, to examine the feasibility of obtaining layers of different properties by changing the technological parameters of the treatment process (laser surface alloying using two types of continuous lasers: an Nd : YAG laser cw-$\lambda = 1.06$ μm and CO_2 cw-$\lambda = 10.6$ μm).

From the viewpoint of applications of the metals under study as a material for electrical contacts, special attention was paid to changes in the microhardness of surface layers obtained by alloying and the improvement of their properties in comparison with base metals, e.g. resistance to erosion in the electric arc.

Microhardness measurements were made by the Vickers method on an "mph 100" microhardness tester constituting the equipment of a NEOPHOT 21 optical

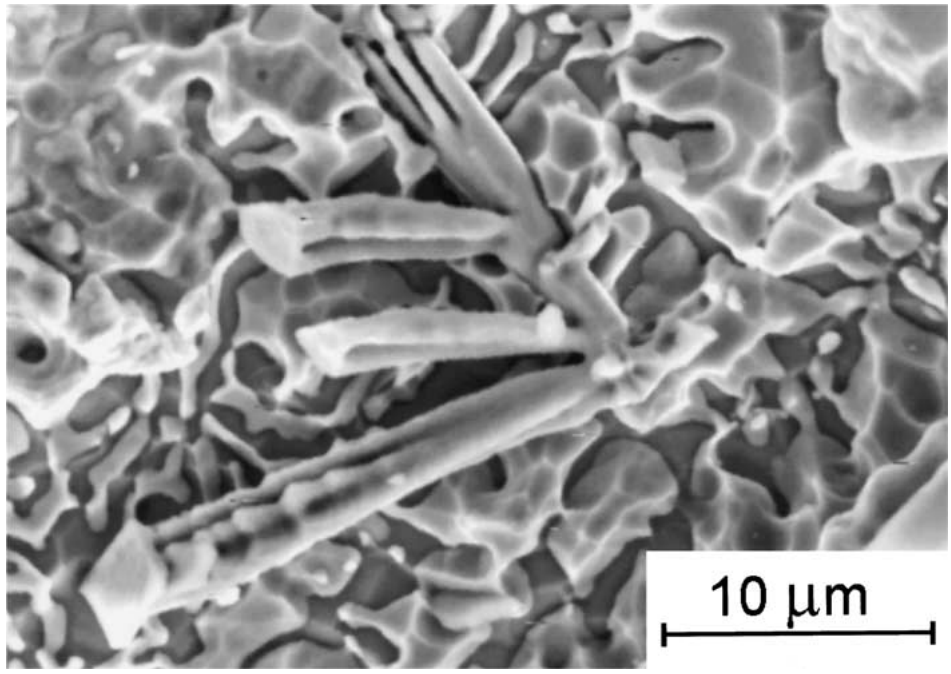

(a)

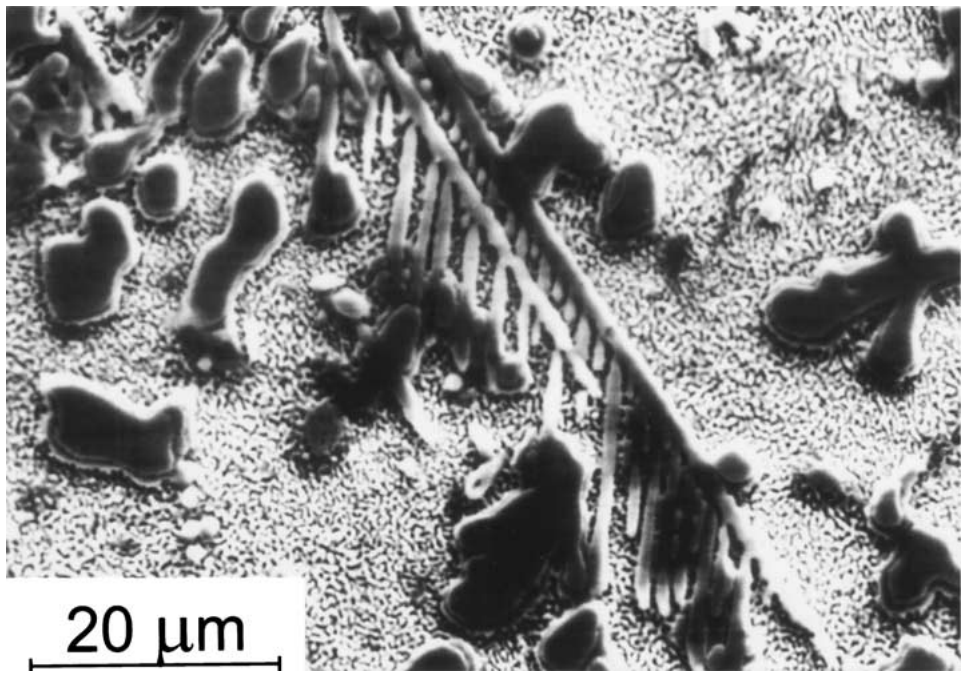

(b)

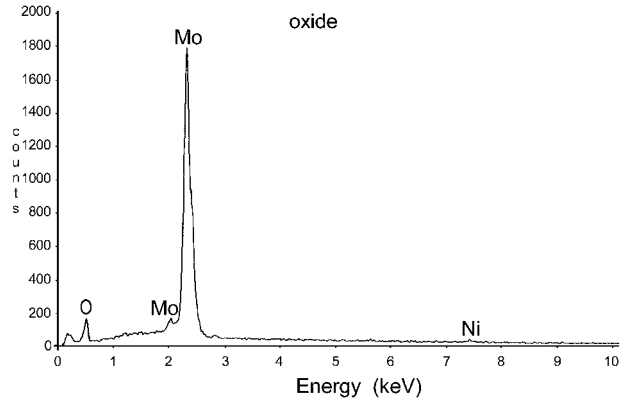

(c)

Figure 3 Dendrites of molybdenum oxides crystallizing in the alloyed ***A*** type layer: (a, b) - a view of oxide dendrites against a background of the eutectic; (c) – an EDX spectrum showing the microanalysis of the dendrite composition.

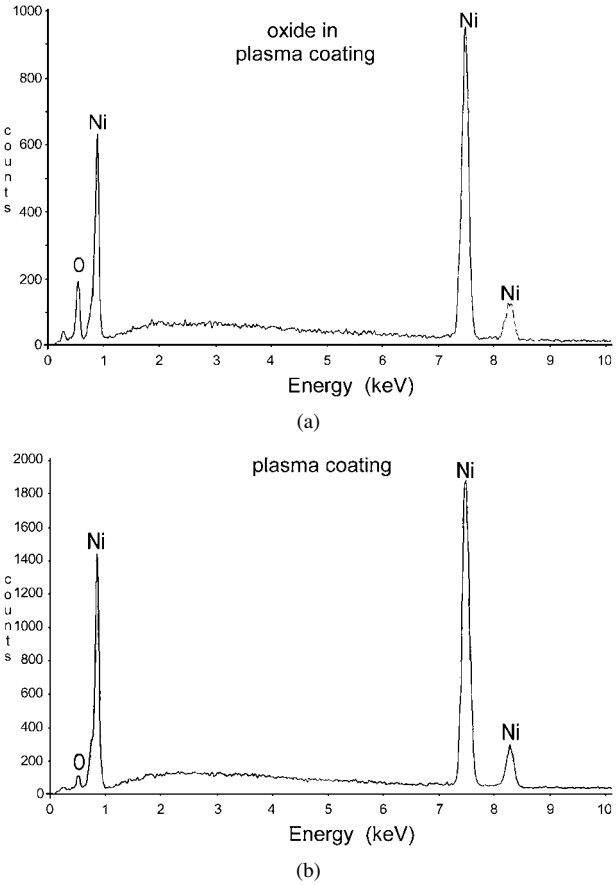

Figure 4 The results of an EDX microanalysis of a plasma sprayed Ni layer: (a) – the composition of Ni oxides in the layer; (b) – the average composition of the layer.

TABLE II The microhardness of structural constituents

Kind of structural constituent	Microhardness of structural constituent, kG/mm^2	
	A-type layer	***B***-type layer
Mo (base metal)	241	222
Dendrite	710	850
Eutectic	905	757
Spheroidal regions	—	1060
Average microhardness	860	770

microscope. Measurement indentations were made on metallographic specimens both while and after etching. The results are shown in the Table II.

Mo-Ni layers are characterized by a very high microhardness, of 860 kG/mm^2 on average for ***A*** type layers and 770 kG/mm^2 for ***B*** type layers. The results of measurements of microhardness of individual constituents of the structure reflect their structure and composition. The dendrites in ***B*** type layers are composed of a more supersaturated Mo-Ni solution (4–8 at % Ni) than those in the ***A*** type layer (2–5 at % Ni) and manifest a greater hardness (850 kG/mm^2 as compared with 710 kG/mm^2). On the other hand, the eutectic phase manifests a greater hardness in ***A*** type layers, since it is more refined (cf. Fig. 2); moreover, its light plates contain more molybdenum (48 at %). The greatest value of microhardness is manifested by spheroidal fragmentations of a complex structure, containing a considerable number of oxide phases (cf. Fig. 6).

TABLE III Electrical parameters of the testing system

Proof voltage	Proof current	Contact time	Arcing time	Contact pressure	Opening rate of the contact
200 V AC	60 A	100 ms	$\leq$10 ms	30 N	1 m/s

Laser-alloyed specimens with ***A*** and ***B*** type surface layers and comparative specimens made of a base metal (Mo) were investigated in a special test station, allowing the measurements of characteristic parameters of the materials used for electric contacts [15]. An image of a laser-welded Mo-Ni contact tip is shown in Fig. 7.

Resistance to erosion in an electric arc (mass loss of the contacts) and contact resistance were assessed. The basic parameters of the investigation are listed in Table III.

10 pairs of contacts with an alloyed Mo-Ni surface layer and 10 pairs of Mo contacts for comparative purposes were investigated. The averaged results of investigation of the erosion wear of the contacts with a type ***A*** laser-alloyed surface layer (Nd : YAG laser) are shown in Fig. 8. The investigations were carried out up to about 1.1×10^5 switching operations until the wear of the laser-modified layer reached approx. 60–70% of its thickness. An analysis of the diagrams shown in Fig. 8a points to a greater initial wear of the contacts with an alloyed surface layer, which, however, stabilizes after about 3×10^4 switching operations. As the test proceeds, the wear of contacts with Mo-Ni layer decreases compared with that of pure Mo contacts. A similar tendency in terms of the function of the number of switching operations is manifested by the change in the contact height (presented elsewhere) for Mo-Ni and Mo contacts. Moreover, the measurement of contact mass for each type of contact, after a specified number of switching operations, revealed a markedly smaller scatter between the smallest and greatest value of mass loss for contacts with a laser-alloyed surface compared with Mo contacts. These results are presented in Fig. 8b as a dependence of a relative scatter of mass loss as a function of the number of switching operations.

The erosion wear of the contact material results from complex relationships between physical phenomena accompanying the start and suppression of an electric arc and the metallurgical processes brought about by the former. Modern contact materials in air-break switching devices can be included among one of the four groups: silver-metal oxide, silver-nickel, silver-carbon and silver-tungsten [16]. In all of these, practically no solubility of the constituents in the solid state in ambient temperature is observed, although such solubility can occur in the liquid state. The individual constituents play different roles when interacting with the contact material of the switching arc; in addition, erosion resistance depends on the morphology of particular phases and such factors as the type of electrical load and the rate of cooling. Generally speaking, the presence of oxide phases has a positive effect on the erosion resistance of contact material, by absorbing the energy during the

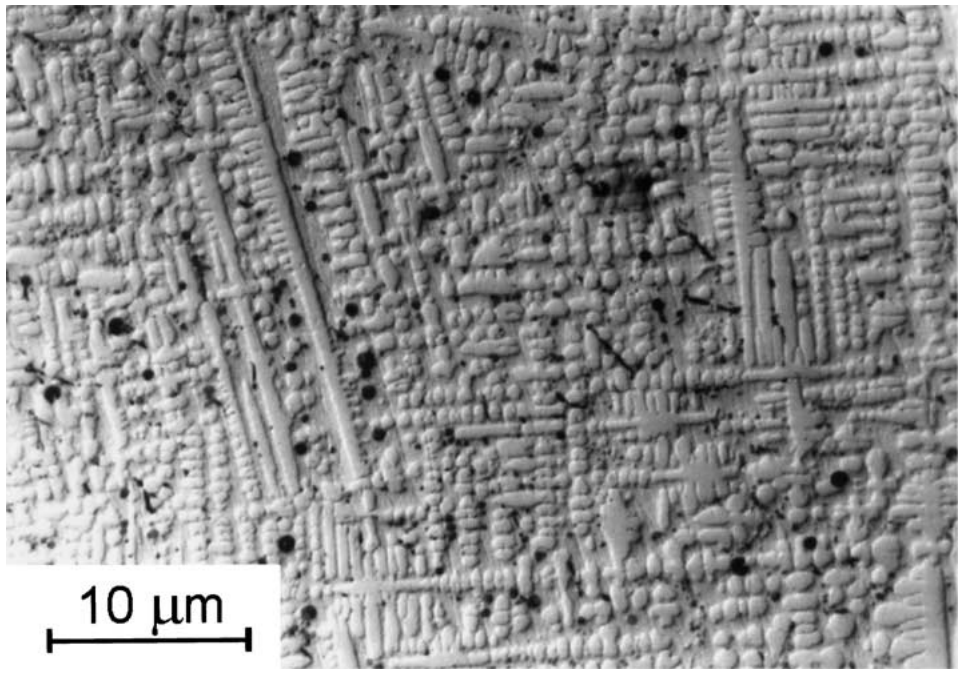

(a)

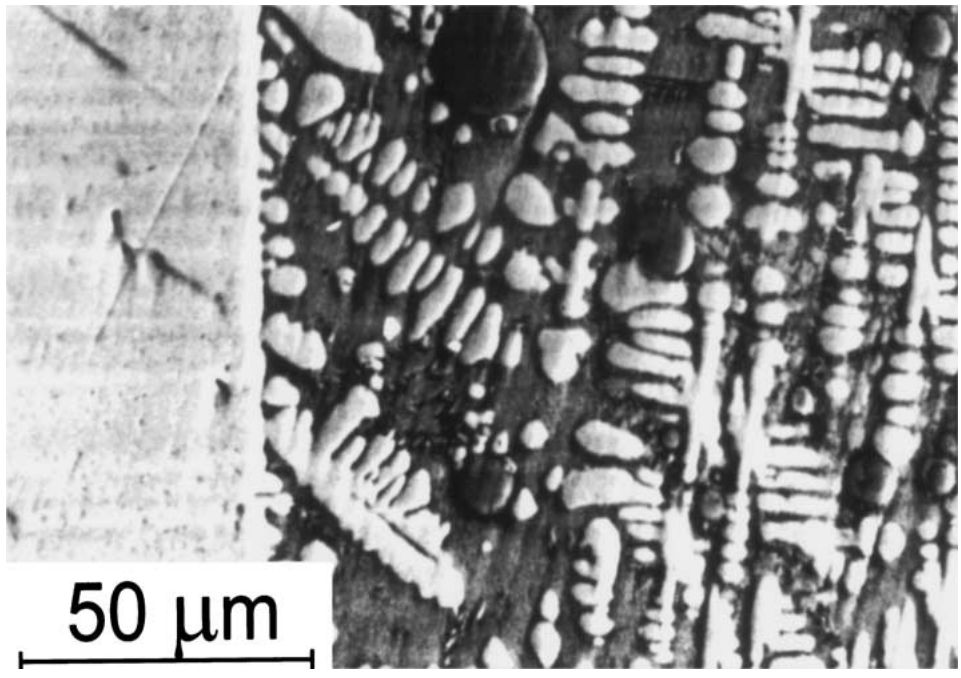

(b)

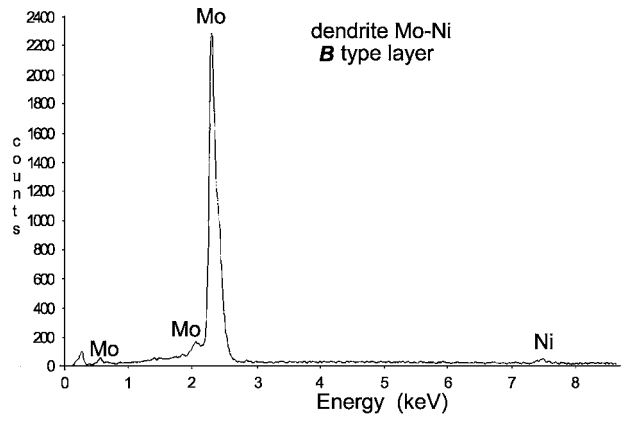

(c)

Figure 5 The structure of B type layers: (a) – a homogeneous dendritic structure; (b) – a 'white' layer of the supersatured solid solution on the boundary with the base; (c) – the EDX spectrum indicating the composition of non-equilibrium dendrites; (d) – an eutectic mixture in the interdendritic space *(Continued)*.

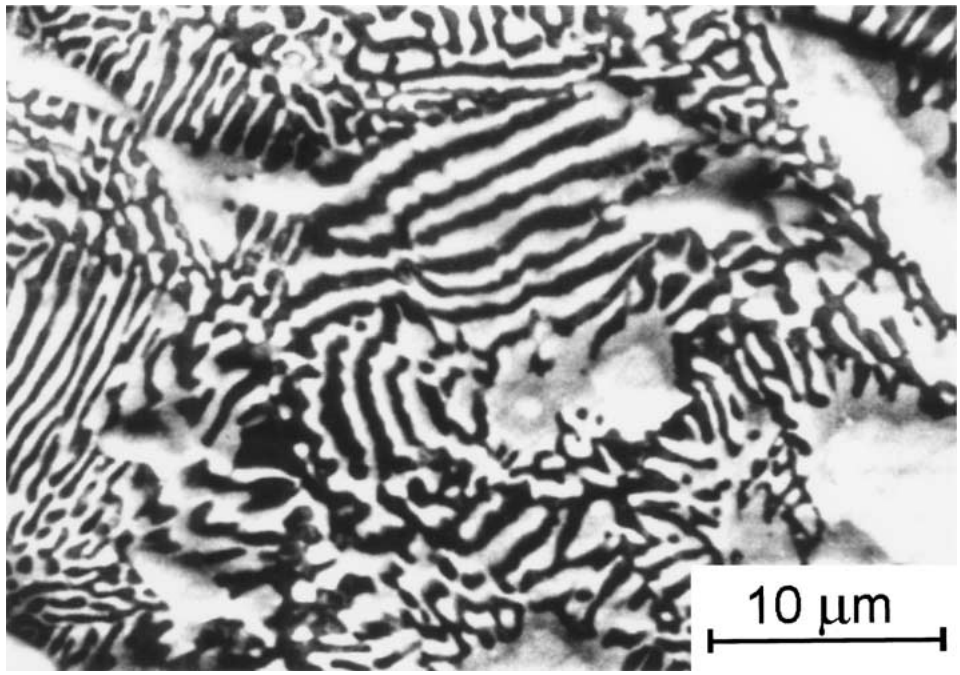

(d)

Figure 5 (Continued).

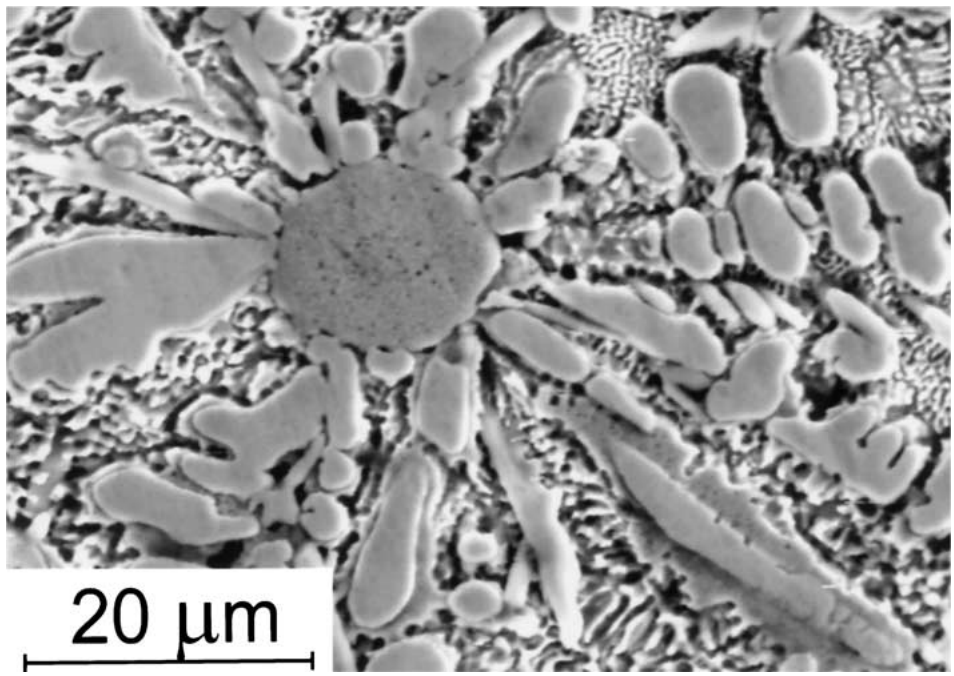

(a)

Figure 6 Spherical regions of a complex structure in the alloyed Mo-Ni layers produced with a CO_2 laser *(Continued).*

decomposition reaction caused by the high temperature of the arc and increasing the viscosity of the fusion formed on the surface of the contact. The presence of the second metallic component has a favourable effect on erosion resistance due to the solubility in the liquid state in the second metal and re-precipitation while cooling, as is the case with Ag-Ni materials, which are produced by powder metallurgy methods. Laser alloying of the surface layer was also used to produce Ag-Ni materials, and their arc erosion resistance was increased [6].

The detailed interpretation of Mo-Ni contact behaviour, compared to Mo contacts, requires further research. As has been shown above, the Mo-Ni layer studied, formed by laser alloying, contain dispersed eutectic, the non-equilibrium phase, a supersaturated solution of nickel in molybdenum and an oxide, MoO_2.

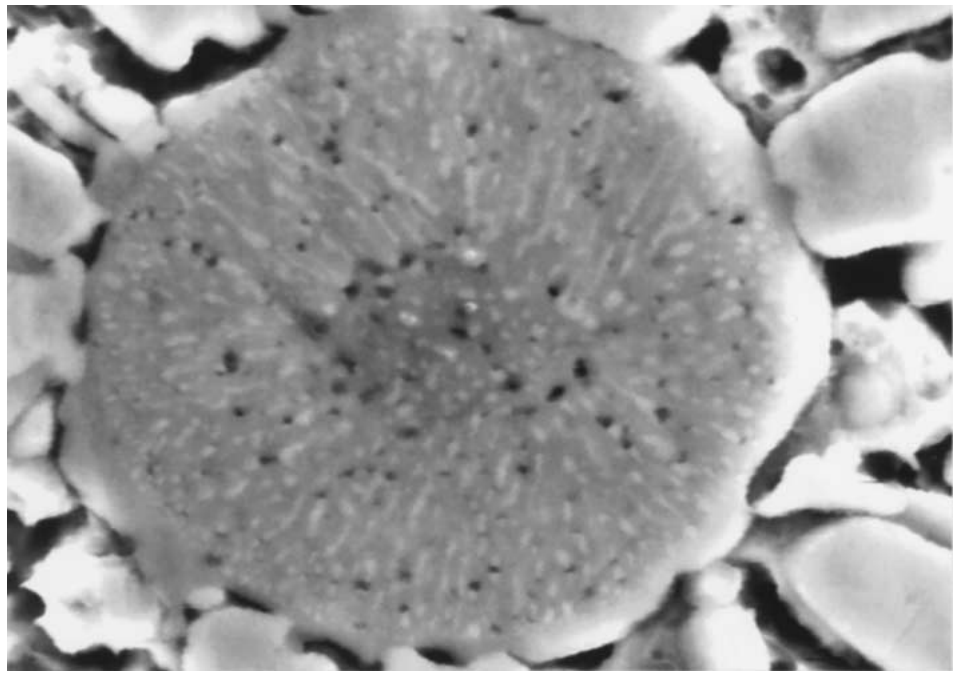

(b)

Figure 6 (Continued).

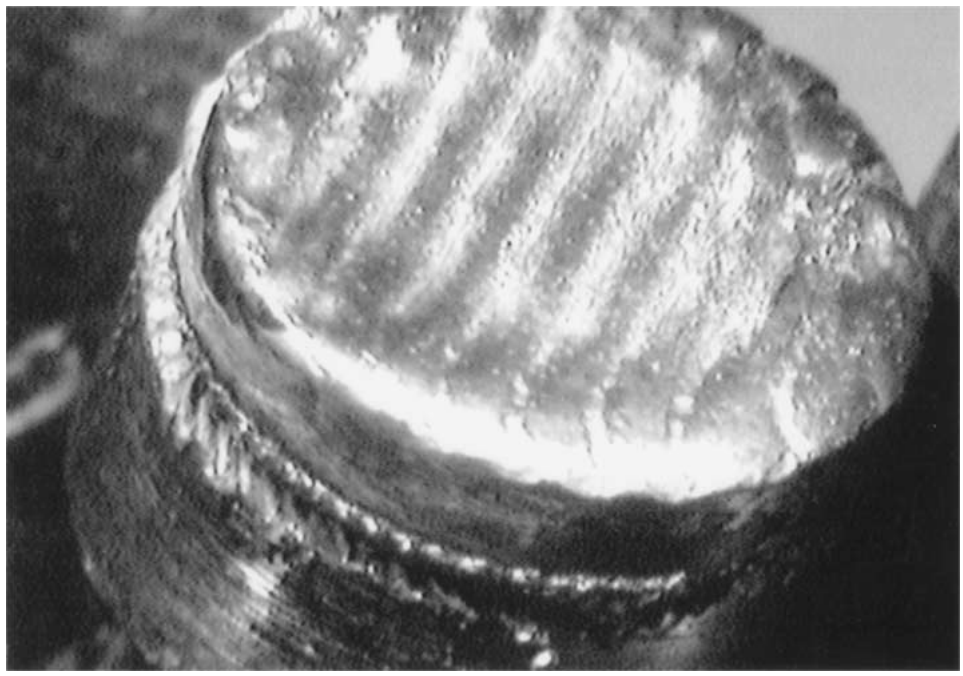

Figure 7 A view of a contact tip with an Mo-Ni surface layer; visible paths after the alloying process using an Nd : YAG laser (***A*** type lasers).

Not all the physical-thermal parameters of these phases are well-known. However, the high temperature generated on the contact surface by the arc foot will definitely cause the decomposition of the non-equilibrium phase and the formation of a liquid solution of nickel in molybdenum. These factors reduce the effects of erosion due to energy absorption. The oxide, MoO_2, decomposes at a temperature of above 850°C, while the decomposition energy is as much as 131 kcal/mole. Thus, the presence of the oxide phase has also a favourable effect on the decrease in erosion. As for the greater initial losses of material, these could be caused by a high content of oxides in the surface layer, which in turned resulted in – found experimentally – an increase in contact resistance, hence the greater temperature of the closed contact. Macro-fractures present in the alloyed layer had also an unfavourable effect on the erosion in the first stage of the test (approx. 0.2×10^5 switching operations). The more stable behaviour of the whole group of Mo-Ni contacts under investigation, compared with Mo contacts (Fig. 8b), may be attributed to the more homogeneous and finely dispersed structure of the alloyed layer. So the microstructure allowed easy migration of the arc foot and prevented the formation of deep craters on the surface as a result of a single start of the arc.

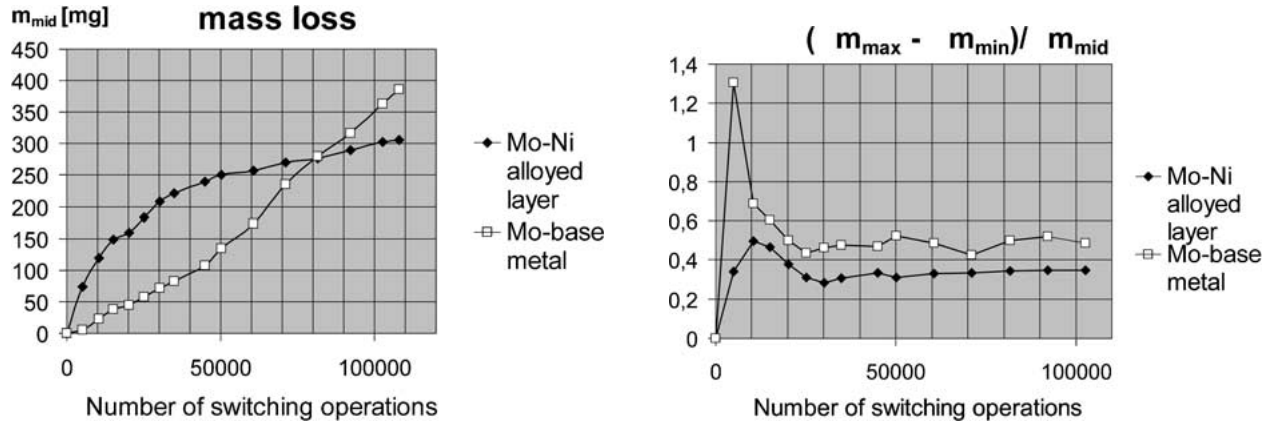

(a) (b)

Figure 8 The erosion behavior of Mo-Ni contacts with a laser-modified surface layer versus Mo contacts (base metal); (a) - erosion losses; (b) - stability of mass losses.

6. Conclusions

In the process of laser-alloying of molybdenum with nickel using a continuous beam of Nd : YAG and CO_2 lasers, a relatively great depth of the layer can be obtained, of an order of 200–500 μm of a high nickel content; however, a strong focusing of the beam is required to obtain this result.

Homogeneous layers containing non-equilibrium phases in the whole volume were obtained while being alloyed by means of a CO_2 laser. The use of an Nd : YAG cw laser, where successive paths overlapped, allows layers of a periodically variable content of nickel to be obtained.

Due to rapid cooling there occurs non-equilibrium crystallization as a result of which, a strongly supersaturated ε phase is formed. The rate of crystallization, to which – in this case – steep temperature gradients contribute, is confirmed by the general dispersion of the structure (of dendrites and eutectics). MoO_2 oxides appeared in the layers, and it is considered that the oxygen was derived from the decomposition of nickel oxides formed during the plasma spraying of a preparatory layer of the alloying material (Ni). The presence of oxides in the plasma sprayed coating could influence the kinetics of solidification. The alloyed layers are characterized by a very high hardness (770–860 kG/mm^2).

The tests aiming at an assessment of the properties of the layers alloyed as possible materials for electric contacts or electrodes do not give a clear answer as to whether such a solution will bring any advantages. Further research is necessary, using other single or, simultaneously, several alloying materials. However, attention should be drawn to the fact of the stable and decreasing wear of the alloyed layers in an electric arc as a function of the number of switching operations, which undoubtedly is related to the very fine-grained microstructure containing non-equilibrium and oxide phases.

References

1. W. STEEN, "Laser Material Processing" (Springer Verlag, 1996).
2. J. SINGH, in "Materials and Processes for Surface and Interface Engineering," edited by Y. Pauleau (Kluwer Academic Publishers, 1995) p. 347.
3. A. GASSER, D. HOFFMANN, F. JANSEN, E. W. KREUTZ, E. LUGSCHEIDER and K. WISSENBACH, *Surface and Coatings Technology* **45** (1991) 409.
4. K. WANG, J. LIU and D. HAN, *Surface Engineering* **12** (1996) 235.
5. S. SASAKI, *ibid.* **13** (1997) 238.
6. R. PAWLAK and T. RACZYŃSKI, *Mater. Sci. Engng.* **A168** (1993) 67.
7. F. KOSTRUBIEC, R. PAWLAK and M. WALCZAK, in "Laser Technology V: Applications in Materials Sciences and Engineering," edited by W. Wolinski and J. Kusinski, Proc. SPIE 3187 (Bellingham, 1997) p. 35.
8. Y. Q. YAN, J. SENKARA and W. WŁOSIŃSKI, *Surface and Coatings Technology* **48** (1991) 211.
9. J. SENKARA, *J. Mater. Sci. Lett.* **10** (1991) 1078.
10. J. M. PELLETIER, L. RENAUD and F. FOUQUET, *Mater. Sci. Engng.* **A134** (1991) 1283.
11. M. GREMAUD, M. CARRARD and W. KURZ, *Acta Metall. Mater.* **38** (1990) 2587.
12. W. KURZ and R. TRIVEDI, *Acta Metall. Mater.* **38** (1990) 1.
13. A. KAR and J. MAZUMDER, *ibid.* **40** (1992) 1873.
14. S. MROWEC, "Theory of Oxidation of Metals and Alloys" (WNT Warszawa, 1964) (in Polish).
15. E. WALCZUK, in Proceedings of the 38th IEEE Holm Conference on Electrical Contacts (Philadelphia, 1992) p. 1.
16. R. MICHAL and K. E. SAEGER, *IEEE Trans. Comp., Hybrids, Manuf. Technol.* **12** (1989) 71.

Received 21 March
and accepted 26 December 2000